Aquaculture xxx (xxxx) xxx

Contents lists available at ScienceDirect

Aquaculture

journal homepage: www.elsevier.com/locate/aquaculture

A truncated peptide Sp-NPFin from the neuropeptide FII SpNPFII of *Scylla paramamosain* exhibiting potent antimicrobial activity

Hua Zhang [a,1], Ying Yang [a,1], Xuewu Zhu [a], Yangzhou Liu [a], Fangyi Chen [a,b,c,*], Ke-Jian Wang [a,b,c,*]

[a] State Key Laboratory of Marine Environmental Science, College of Ocean and Earth Sciences, Xiamen University, Xiamen, Fujian, China
[b] State-Province Joint Engineering Laboratory of Marine Bioproducts and Technology, College of Ocean and Earth Sciences, Xiamen University, Xiamen, Fujian, China
[c] Fujian Collaborative Innovation Center for Exploitation and Utilization of Marine Biological Resources, College of Ocean and Earth Sciences, Xiamen University, Xiamen, Fujian, China

ARTICLE INFO

Keywords:
Neuropeptide FII (SpNPFII)
Sp-NPFin
Scylla paramamosain
Antimicrobial activity
Antimildew activity

ABSTRACT

Neuropeptide (NP) F is a homolog of vertebrate neuropeptide Y, and mounting evidence suggests that it may play a role in innate immunity in addition to its function in invertebrate neurobiology. However, so far, there have been few reports on the immunological properties of crustacean NPs. Here, we cloned a neuropeptide FII gene, naming it SpNPFII, from the mud crab *Scylla paramamosain*. The full-length cDNA sequence of SpNPFII was 551 bp, encoding 124 amino acids. Structural prediction suggested that the SpNPFII mature peptide mainly formed an α-helix. SpNPFII was predominately expressed in male crab gonadal tissues, with the highest expression in the anterior vas deferens and seminal vesicle. The expression level of SpNPFII changed significantly under challenge by lipopolysaccharide (LPS) or *Vibrio alginolyticus*. After bioinformatic analysis, a truncated 45-amino acid peptide derived from SpNPFII and having potent antimicrobial activity was identified and named Sp-NPFin. Sp-NPFin exerted strong, broad-spectrum antibacterial (minimum inhibitory concentration [MIC] ranged from 1.5 to 12 μM) and antimildew activity (MIC ranged from 1.5 to 48 μM), a low fungicidal concentration (*e.g.*, minimum bactericidal concentration [MBC] for *Fusarium oxysporum* was 1.5 to 3 μM) and rapid bactericidal kinetic (killed all bacteria within 1 to 6 h). Sp-NPFin could bind to several microbial surface components (*e.g.* LPS, lipoteichoic acid, peptidoglycan and glucan), and induce significant damage to microbial membranes and cause leakage of cell contents in a concentration-dependent manner. Confocal microscopy indicated that Sp-NPFin was localized at microbial surfaces. In addition, Sp-NPFin exhibited no cytotoxicity to primary cultured crab hemocytes and mammalian cells, and *in vivo* study demonstrated that it could significantly improve the survival rate of *S. paramamosain* under the challenge of *V. alginolyticus*. Taken together, SpNPFII might play a role in the immune system of *S. paramamosain*, and its truncated peptide, Sp-NPFin, would be a promising antibacterial and antimildew agent with broad application prospects in the fields of aquaculture, veterinary practices and medicine.

1. Introduction

Neuropeptides (NPs) are a class of endogenous peptides synthesized and released by neurons, and are involved in a variety of physiological processes (Merighi, 2011). The first NP to be identified, substance P, was discovered in 1931 but not reported until 1971 (Chang et al., 1971). As one of the most complete NP databases, NeuroPep (http://isyslab.info/NeuroPep/home.jsp) has collected 5949 non-redundant NPs from 493 organisms in 65 neuropeptide families, mainly from the allatostatin family, Gastrin family, endogenous opioid peptide family, tachykinin family and neuropeptide Y (NPY) family. Over the past decades, studies have confirmed that NPs are widely distributed and play roles in almost all aspects of daily life, including but not limited to reproduction, feeding, ageing, learning, and memory (Jenwitheesuk et al., 2017; Matsuda et al., 2015; Nässel and Zandawala, 2019; Shao et al., 2016; Sharma et al., 2018). In addition, considerable evidences supports

* Corresponding authors at: College of Ocean and Earth Sciences, Xiamen University, Xiamen, Fujian 361102, PR China.
E-mail addresses: chenfangyi@xmu.edu.cn (F. Chen), wkjian@xmu.edu.cn (K.-J. Wang).
[1] These authors made equal contributions.

https://doi.org/10.1016/j.aquaculture.2020.736145
Received 31 August 2020; Received in revised form 15 October 2020; Accepted 7 November 2020
Available online 12 November 2020

bidirectional crosstalk between the neuroendocrine system and the immune system, suggesting that NPs may regulate immune responses at different levels as pleiotropic modulators (Augustyniak et al., 2012; Brogden et al., 2005; Delgado and Ganea, 2008; Metz-Boutigue et al., 2003; Nguyen et al., 2002).

The neuropeptide Y family is one of the most widely studied NP families, including NPY, peptide YY (PYY), and pancreatic polypeptide (PP) in vertebrates, and neuropeptide F (NPF) in invertebrates (Takei, 2016). Studies have shown that these peptides, especially NPY, play pivotal roles in many physiological and pathophysiological processes (Augustyniak et al., 2012; Botelho and Cavadas, 2015; Brogden et al., 2005; Duarte-Neves et al., 2016; Ramos et al., 2005; Reichmann and Holzer, 2015). There is growing evidence that NPY is involved in mediating the inflammatory response of intestinal physiology, Parkinson's disease (PD) and asthma (Lu et al., 2015; Pain et al., 2019; Sanz and Aidy, 2019). In a mouse model of polytropic retrovirus infection, NPY reduces retrovirus-induced neurological disease by suppressing the recruitment of monocytes into the brain (Woods et al., 2016). Additionally, NPY could increase phagocytosis of *Candida albicans* by murine peritoneal phagocytes (Bedoui et al., 2007). Finally, studies have reported direct antimicrobial activities of NPY against *Escherichia coli*, *Cryptococcus neoformans* and *Arthroderma simii*, with a minimal inhibitory concentration (MIC) value less than 10 μM (Augustyniak et al., 2012). All these studies point to the significant role of NPY in the innate immunity of vertebrates.

NPF is a homolog of NPY in invertebrates. The first NPF was identified in the tapeworm *Monieza expansa* (Maule et al., 1991), and subsequently characterized in many other invertebrates (Nässel and Wegener, 2011). The most extensively studied functions of NPF in *Drosophila* include foraging, feeding and motivation, ethanol sensitivity, stress response (*e.g.*, nociception, aggression, reproduction, clock function and learning) (Nässel and Wegener, 2011). However, there are few reports on NPF in crustaceans. In Pacific white shrimp (*Litopenaeus vannamei*), NPF was shown to regulate feeding and food intake (Christie et al., 2011). In female freshwater prawns (*Macrobrachium rosenbergii*), NPF could affect ovarian maturation and spawning (Tinikul et al., 2017). In the mud crab *Scylla paramamosain*, NPF, along with other NPs, was first discovered by a large-scale RNA sequencing of female crab cerebral ganglia. The expression level of NPF was significantly up-regulated at the early vitellogenic stage, but down-regulated at the late vitellogenic stage compared to the pre-vitellogenic stage, indicating the role of NPF in ovarian maturation (Bao et al., 2015). However, there are no additional reports on its function, let alone its role in innate immunity. The question of whether the NPF in *S. paramamosain*, like other vertebrate NPY family members, also function as a pleiotropic modulator in the immune response, has attracted us to further explore this topic.

In this study, based on the transcriptome database of *S. paramamosain* established by our laboratory, the full-length cDNA sequence of the NPFII gene was cloned and named SpNPFII. The expression profiles of SpNPFII in *S. paramamosain* under LPS or *Vibrio alginolyticus* challenges were investigated. Based on bioinformatic analysis of SpNPFII, we chemically synthesized a truncated peptide derived from SpNPFII, named Sp-NPFin, and determined its antimicrobial activity *in vitro*. Following the antimicrobial activity assay, scanning electron microscopy (SEM), transmission electron microscopy (TEM), confocal laser scanning microscopy (CLSM) observations and microbial surface components binding assays were employed to investigate the antimicrobial activity of Sp-NPFin on various microorganisms *in vitro*. Moreover, the *in vivo* protective activity of Sp-NPFin was further evaluated using *V. alginolyticus* infected *S. paramamosain*.

2. Materials and methods

2.1. Microorganism strains and reagents

The strains, including *Staphylococcus aureus* (CGMCC1.2465), *S. epidermidis* (CGMCC1.4260), *Escherichia coli* (CGMCC1.2389), *Pseudomonas aeruginosa* (CGMCC1.2421), *V. harveyi* (CGMCC1.1593), *V. fluvialis* (CGMCC1.1609), *V. alginolyticus* (CGMCC1.1833), *V. parahaemolyticus* (ATCC®33846), *C. neoformans* (CGMCC2.1563), *C. albicans* (CGMCC2.2411), *P. stutzeri* (CGMCC1.1803), *P. fluorescens* (CGMCC1.3202), *Shigella flexneri* (CGMCC1.1868), *Bacillus subtilis* (CGMCC1.3358), *Corynebacterium glutamicum* (CGMCC1.1886), *Fusarium oxysporum* (CGMCC3.6785), *F. solani* (CGMCC3.584), *Aspergillus niger* (CGMCC3.316), *A. fumigatus* (CGMCC3.5835), and *A. ochraceus* (CGMCC3.583) were purchased from CGMCC (China General Microbiological Culture Collection Center, Beijing, China). *Pichia pastoris* (GS115) was purchased from Invitrogen (Thermo Fisher Scientific, USA). Multi-drug resistant bacteria strains isolated from clinical samples, including *Acinetobacter baumannii* QZ18050, *Klebsiella pneumoniae* QZ18107, *E. coli* QZ18109, *P. aeruginosa* QZ19125, *Enterococcus faecium* QZ19080 and *S. aureus* QZ18090 were kindly provided by the 2nd Affiliated Hospital of Fujian Medical University (Quanzhou, Fujian, China). Yeasts were cultured in Yeast Extract Peptone Dextrose (OXOID, UK) agar at 28 °C, vibrios were cultured in Marine Broth 2216 Medium agar (BD DIFCO, USA) at 28 °C, and other strains were cultured in nutrient broth medium (OXOID, UK) agar at 37 °C. L02 (HL-7702) and HEK293T (ATCC ® CRL-3216) were purchased from the Chinese Academy of Sciences (Shanghai, China). Lipopolysaccharides (LPS) from *E. coli* 055: B4, lipoteichoic acid (LTA) from *Bacillus subtilis*, peptidoglycan (PGN) from *B. subtilis* and glucan from baker's yeast were purchased from Merck, Germany. Mouse anti-His antibody, Goat Anti-Rabbit IgG Antibody conjugated with horseradish peroxidase were purchased from Beijing Zhongshan Jinqiao Biotechnology Co., Ltd., China. Goat anti-Rabbit IgG (H + L) secondary antibody (Dylight 650) and 4′,6-diamidino-2-phenylindole dihydrochloride (DAPI) were purchased from Thermo Fisher Scientific Co. CellTiter 96™ AQueous One Solution Cell Proliferation Assay Kit, were obtained from Promega Co.

2.2. Animals, challenge and tissue collection

Mud crabs (*S. paramamosain*) were purchased from the Zhangpu Fish Farm (Fujian, China), and were allowed to acclimate for 3 days before experiments. Before sampling, the crabs were anesthetized by ice-bathing for 15 min, and all efforts were made to minimize their suffering. Tissues were dissected using sterile tools, and flash frozen in liquid nitrogen and stored at −80 °C until use. All animal experiments were carried out in strict accordance with the guidelines of Xiamen University. To investigate the natural *in vivo* expression profile of SpNPFII, healthy male and female adult mud crabs (bodyweight 300 ± 30 g, n = 3) were dissected, and tissues including testis, anterior vas deferens, seminal vesicle, posterior vas deferens, ejaculatory duct, posterior ejaculatory duct, penis, ovary, spermathecae, reproductive duct, muscle, thoracic ganglion, gills, brain, midgut, subcuticular epidermis, eye stalk, heart, hepatopancreas and stomach were collected. Hemocytes were isolated from the hemolymph as described previously (Chen et al., 2010). For the LPS-challenge experiment, adult male crabs (bodyweight 300 ± 30 g, n = 5) were injected with LPS (prepared in crab saline: NaCl, 496 mM; KCl, 9.52 mM; $MgSO_4$, 12.8 mM; $CaCl_2$, 16.2 mM; $MgCl_2$, 0.84 mM; $NaHCO_3$, 5.95 mM; HEPES, 20 mM; pH 7.4) at a dosage of 0.5 mg kg^{-1}. For the *V. alginolyticus* challenge experiment, male crabs (body weight 300 ± 30 g, n = 5) were injected with *V. alginolyticus* (1×10^6 CFU $crab^{-1}$). Crabs injected with crab saline were set up as the control group. Tissue samples (testes and hepatopancreas) were collected at 3, 6, 12, 24 and 48 h post-injection.

2.3. cDNA cloning and bioinformatics analysis

Following the manufacturer's instructions, total RNA of testes was extracted using TRIzol™ reagent (Invitrogen, USA) and cDNA was generated using a PrimeScript™ RT reagent Kit with a gDNA Eraser Kit (Takara, China). The cDNA templates for 5′- and 3′- random amplification of cDNA ends (RACE) PCR were synthesized using a SMARTer® RACE 5′/3′ Kit (Takara, China). Gene-specific primers were designed based on the partial sequences obtained from the transcriptome database established by our laboratory (Table 1). The amplified fragments were cloned into the pMD18-T Vector (Takara, China) and sequenced by Borui biotechnology Ltd. (Xiamen, China). The homology and similarity of the SpNPFII cDNA sequence was analyzed using an online tool from the National Center for Biotechnology Information (NCBI, https://www.ncbi.nlm.nih.gov/). The signal peptide and functional domain were predicted with SignalP 4.1 Server (http://www.cbs.dtu.dk/services/SignalP/) and SMART (http://smart.embl-heidelberg.de/) respectively. The theoretical isoelectric point and molecular weight were calculated using online software (https://web.expasy.org/compute_pi/). The protein structure was predicted and modeled by I-TASSER (https://zhanglab.ccmb.med.umich.edu/I-TASSER/). Multiple sequence alignment was performed using Clustal X 2.1 Software. A neighbor-joining phylogenetic tree was constructed with MEGA5.0, and 1000 bootstraps were selected to evaluate its reliability. The prohormone convertase cleavage site was predicted by NeuroPred (http://neuroproteomics.scs.illinois.edu/neuropred.htm).

2.4. Quantitative real-time PCR

Total RNA was extracted and cDNA was generated as described above. Quantitative real-time PCR (qPCR) was performed on a LightCycler480 (Roche Diagnostics) using FastStart DNA Master SYBR Green I (Roche Diagnostics). The tissue distribution of the SpNPFII transcript was detected by absolute qPCR assay, and the responses of the SpNPFII gene to different stimuli were measured by relative qPCR. For the relative qPCR assay, Sp-GAPDH (GenBank accession number: JX268543.1) was chosen as the reference gene and quantified to normalize the SpNPFII expression. The primer sequences are listed in Table 1. The qPCR cycling condition was set as follows: an initial denaturing step at 95 °C for 5 min, and 40 cycles at 95 °C for 30 s, 60 °C for 30 s and 72 °C for 1 min. Data were analyzed using the algorithm of the $2^{-\Delta\Delta Ct}$ method (Livak and Schmittgen, 2001).

2.5. Design and synthesis of Sp-NPFin

The amino acid sequence of SpNPFII was subjected to SMART analysis (http://smart.embl.de/). The results indicated that the sequence contained a pancreatic hormones (PAH) domain. The sequence was further subjected to the CAMP-R3 server (http://www.camp.bicnirrh.res.in/) to predict fragments (containing the previously predicted PAH domain) that potentially have antimicrobial activity. The predicted sequences were synthesized using solid-phase chemical syntheses by GL Biochem Ltd. (Shanghai, China), and subjected for antimicrobial activity evaluation. A truncated 45-amino acid peptide with the best antimicrobial activity was selected and named as Sp-NPFin. The purity of synthesized Sp-NPFin was over 95%. The synthetic peptide was stored at −80 °C and dissolved in sterile deionized water prior to use.

2.6. Polyclonal antibody preparation

The amino acid sequence of SpNPFII was subjected to the Optimum Antigen design tool for antigen site prediction. Synthesis of the selected antigen site (CIYSHMTRPRFGKRS), and preparation and quality inspection of the antibody were performed by GenScript (NJ, CHN).

2.7. Antimicrobial assay

Microorganisms (as listed in Table 2) were harvested during their logarithmic growth phase, washed with 10 mM Dulbecco's phosphate buffered saline (DPBS, pH 7.4) and adjusted to 3.3×10^4 CFU mL^{-1} (bacteria and yeasts) or 5×10^4 CFU mL^{-1} (mycotic spores) before incubating with serial diluted Sp-NPFin. The minimum inhibitory concentration (MIC) and minimum bactericidal concentration (MBC) of Sp-NPFin were determined in triplicate on separated occasions following a liquid growth inhibition assay protocol described previously (Liu et al., 2017).

2.8. Time-killing kinetic

The Gram-positive bacteria *S. aureus* and Gram-negative bacteria *P. aeruginosa* were subjected to the previously described time-killing study. Briefly, Sp-NPFin was incubated with bacteria (3.3×10^4 CFU mL^{-1}) at concentrations of 24 μM (for *S. aureus*) and 12 μM (for *P. aeruginosa*). The cultures were sampled, diluted and plated at various time points post incubation. The plates were incubated at 37 °C for 18 to 24 h. The total viable count (TVC) was obtained with the standard plate count for bacterial colonies to estimate the population of live microbial load. Killing efficiency was determined following previously published methods (Chen et al., 2010; Liu et al., 2017). The experiments were performed in triplicate.

Table 1
Primer sequences.

Primers	Accession No.	Sequence (5′–3′)
SpNPFII-ORF-F	SpNPFII (MN735439)	ATGTGCCGCCAGCTCCTGACAGCTC
SpNPFII-ORF-R		TCACCGCCTCCTTGCCAGTGTCTCC
SpNPFII-5′-R1		TTGCCAGTGTCTCCAGCAGC
SpNPFII-5′-R2		CGCGGTCTGGTCATGTGTGA
SpNPFII-5′-R3		TGGGGTCTGGTTTGCCCTCT
SpNPFII-3′-F1		GGGCAAACCAGACCCCACTC
SpNPFII-3′-F2		ACATGACCAGACCGCGCTTC
SpNPFII-3′-F3		GGAGGCAAGTGAGAGGCTGC
Long primer	Provided by SMARTer™ RACE cDNA Amplification Kit	CTAATACGACTCACTATAGGGCAAGCAGTGGTATCAACGCAGAGT
Short primer		CTAATACGACTCACTATAGGGC
NUP		AAGCAGTGGTATCAACGCAGAGT
M13-47F	Universal sequencing primers for pMD18-T vector (TaKaRa)	CGCCAGGGTTTTCCCAGTCACGAC
M13-48R		AGCGGATAACAATTTCACACAGGA
SpNPFII -qPCR-F		TCCCCGGTTTCCCGACCCAG
SpNPFII -qPCR-R		ACCAGGAGGCAGCACCGTCT
GAPDH-qPCR-F	GADPH (JX268543.1)	CTCCACTGGTGCCGCTAAGGCTGTA
GAPDH-qPCR-R		CAAGTCAGGTCAACCACGGACACAT

Table 2
Antimicrobial activity of Sp-NPFin.[a, b]

Microorganisms	CGMCC No.[a]	MIC (μM)[b]	MBC (μM)[b]
Gram-negative bacteria			
Escherichia coli	1.2389	3–6	6–12
Pseudomonas aeruginosa	1.2421	6–12	6–12
Pseudomonas stutzeri	1.1803	<1.5	3–6
Pseudomonas fluorescens	1.3202	1.5–3	3–6
Shigella flexneri	1.1868	3–6	3–6
Gram-positive bacteria			
Bacillus subtilis	1.3358	1.5–3	1.5–3
Corynebacterium glutamicum	1.1886	1.5–3	1.5–3
Staphylococcus aureus	1.2465	6–12	12–24
Fungi			
Fusarium oxysporum	3.6785	1.5–3	1.5–3
Fusarium solani	3.584	3–6	3–6
Aspergillus niger	3.316	3–6	6–12
Aspergillus fumigatus	3.5835	3–6	>48
Aspergillus ochraceus	3.583	24–48	>48
Multi-drug resistant bacteria			
Acientobacter baumannii QZ18050	–	1.5–3	3–6
Klebsiella pneumoniae QZ18107	–	1.5–3	1.5–3
Escherichia coli QZ18109	–	3–6	6–12
Pseudomonas aeruginosa QZ19125	–	12–24	12–24
Enterococcus faecium QZ18080	–	3–6	6–12
Staphylococcus aureus QZ18090	–	24–48	24–48

[a] CGMCC No., China General Microbiological Culture Collection Number.
[b] The MIC and MBC values are presented as the interval [A]-[B]: [A] is the highest concentration tested with visible microbial growth, while [B] is the lowest concentration without visible microbial growth (n = 3).

2.9. Binding assays

To determine the binding properties of Sp-NPFin to LPS, LTA, PGN and glucan, a modified enzyme-linked immune sorbent assay (ELISA) was performed following prior method descriptions (Liu et al., 2017). Briefly, a 96-well ELISA plate was coated with LPS, LTA, PGN and glucan (2 μg), blocked with 5% skim milk (prepared in PBS), and incubated with serial dilutions of Sp-NPFin (0 to 80 μg mL^{-1}, prepared in PBS). Bound peptides were detected by incubation with Mouse anti-His antibody (1:3000, prepared in 1% skim milk) followed by Goat Anti-Rabbit IgG Antibody conjugated with horseradish peroxidase (1:5000, prepared in 1% skim milk). After colorimetric reaction, the absorbance at 450 nm was measured using a microplate reader (TECAN GENios). Experiments were carried out in triplicate, and the apparent dissociation constant (K_d) was generated by Scatchard plot analysis.

2.10. Sp-NPFin localization assay

S. aureus, *P. aeruginosa* (5×10^7 CFU mL^{-1}) and mycotic spores *F. oxysporum* and *A. niger* (2.5×10^6 CFU mL^{-1}) were prepared as described for the antimicrobial assays. Sp-NPFin was incubated with the microbial suspensions (24 μM for *S. aureus*, 12 μM for *P. aeruginosa*, and 24 μM for *A. niger*, 6 μM for *F. oxysporum*). Microbial suspensions supplemented with equal volume of PBS (pH 7.4) were set up as control groups. After incubation for 30 min, microorganisms were fixed with 4% paraformaldehyde for 30 min before proceeding to the immunofluorescence detection, as previously described (Liu et al., 2020). Briefly, samples were permeabilized using 0.1% (*v*/v) Triton X-100 (prepared in PBS, pH 7.4) and blocked with 5% bovine serum albumin (BSA, prepared in PBS, pH 7.4) for 1 h at room temperature. Samples were incubated with SpNPFII antibody (1:1000, diluted in 1% [*v*/v] BSA) overnight at 4 °C, washed multiple times with PBS, and incubated with Dylight 650 conjugated goat anti-rabbit IgG (1:1000, diluted in 1% [v/v] BSA) in the dark for 1 h at room temperature. DAPI was applied for chromatin staining. Samples were observed with a confocal laser scanning microscope (CLSM, Zeiss Lsm 780 NLO, Germany).

2.11. SEM and TEM assays

For electron microscopy examination, *S. aureus*, *P. aeruginosa* (5×10^7 CFU mL^{-1}) and mycotic spores *F. oxysporum* and *A. niger* (2.5×10^6 CFU mL^{-1}) were prepared as described for the antimicrobial assay. Sp-NPFin was supplemented into microbial suspensions and incubated for different time-periods (*S. aureus*: 24 and 48 μM, 10 min; *P. aeruginosa*: 12 and 24 μM, 30 min; *A. niger*: 12 and 24 μM, 60 min; *F. oxysporum*: 3 and 6 μM, 60 min). Microbial suspensions were collected and fixed with pre-cooled 2.5% glutaraldehyde at 4 °C for 2 h. For SEM (SUPRA 55 SAPPHIRE, Carl Zeiss, Germany) observations, samples were first dehydrated and gold-sputtered (Lin et al., 2013). For TEM (FEI Tecnai G2 F20) observations, samples were subjected for ultrathin sectioning and were negatively stained following standard protocols (Chen et al., 2003).

2.12. Cytotoxicity assay

The potential cytotoxicity of Sp-NPFin was evaluated using hemocytes of *S. paramamosain*, L02 and HEK-293 T cells. The hemocytes of *S. paramamosain* were prepared as previously described (Deepika et al., 2014; Qiao et al., 2014). Briefly, hemocytes were collected from live animals, seeded at 10^4 cells $well^{-1}$ on a 96-well cell culture plate, and cultured overnight at 26 °C in L-15 medium prepared in crab saline and supplemented with 5% fetal bovine serum (FBS). L02 and HEK-293 T cells were seeded at 10^4 cells $well^{-1}$ on a 96-well cell culture plate and incubated overnight at 37 °C in a humidified atmosphere with 5% CO_2. Cells were incubated in a culture medium supplemented with various concentrations of Sp-NPFin (3, 6, 12, 24 and 48 μM) for 24 h. Cell viability was assessed using a CellTiter 96® AQueous Kit (Promega). Experiments were carried out in triplicate.

2.13. Evaluation of the in vivo activity of Sp-NPFin on S. paramamosain infected with V. alginolyticus

To investigate the *in vivo* activity of Sp-NPFin, we performed a mortality comparison using male *S. paramamosain* (body weight 40 ± 5 g) infected with *V. alginolyticus*. Sp-NPFin and the pathogenic bacterium *V. alginolyticus* were prepared in crab saline for the experiments. First, *V. alginolyticus* (2×10^5 CFU $crab^{-1}$) were injected into the base of the right fourth leg of the crabs. Sixty crabs infected with bacteria were divided into two groups (control group and treatment group) with 30 crabs in each group. Then, 6 h after the bacterial injection, Sp-NPFin (40 μg $crab^{-1}$) was injected into the crabs as the treatment group, and an equal volume of crab saline was injected into the crabs for the control group. The survival rates of crabs were recorded at different time points (12, 24, 36, 48, 60 and 72 h).

2.14. Statistical analysis

Results are presented as the mean ± standard deviation (SD). For the absolute qPCR assays, one-way analysis of variance (ANOVA) followed by a Turkey post-test were applied to compare the expression levels of SpNPFII in different tissues of *S. paramamosain.* For the relative qPCR assays, two-way ANOVA followed by a Bonferroni post-test were applied to compare the expression levels of SpNPFII before and after treatments. For cytotoxicity assays, one-way ANOVA followed by a Dunnett post-test were applied to compare the cell viability of Sp-NPFin treatment and control groups. For mortality comparison, data were analyzed using the Kaplan-Meier Log rank test. Statistical analysis was performed using GraphPad Prism 6.0 Software (GraphPad Software Inc., CA, USA). Differences were accepted as significant at $p < 0.05$.

3. Results

3.1. Cloning and sequence analysis of SpNPFII

The full-length cDNA sequence of SpNPFII was 551 bp with a 375 bp open reading frame (ORF), encoding 124 amino acids (GenBank accession number: MN735439). SpNPFII had its signal peptide cleaved at the N-terminus between Gly-26 and Lys-27 (Fig. 1A). The mature peptide of SpNPFII contained 72 amino acid residues, with a total hydrophobic ratio of 31%. The total net charge of SpNPFII was +6.75, suggesting that it was a cationic peptide. The calculated mass of the SpNPFII mature peptide was 8.2 kDa, with an estimated isoelectric point (p*I*) of 10.46. Three-dimensional structure prediction results showed that the SpNPFII mature peptide mainly formed an α-helical structure (Fig. 1C). The multiple sequence alignment (Fig. 1D) and NJ tree (Fig. 1B) were constructed to perform an evolutionary relationship analysis of SpNPFII with the NPF/NPY from *S. paramamosain* and other species. As shown in Fig. 1B, the phylogenetic tree was divided into two groups. Cluster II included mainly vertebrate NPY. SpNPFII was clustered in group I with NPF from other invertebrates, possessing a close evolutionary relationship to the giant freshwater prawn (*Macrobrachium rosenbergii*).

3.2. Gene expression profiles of SpNPFII

The qPCR results showed that transcriptional expression levels of SpNPFII varied among different tissues. In male adult crabs, SpNPFII was dominantly expressed in sexual gonads with the highest expression levels observed in the anterior vas deferens and seminal vesicle (Fig. 2A). Relatively low expression levels of SpNPFII were observed in female adult crabs (Fig. 2D). We further investigated the expression profiles of SpNPFII in testes and the hepatopancreas of male crabs after LPS or *V. alginolyticus* challenge (Fig. 2B, C, E and F). In testes, SpNPFII expression was significantly induced by LPS challenge at 3- and 48-h post-injection (Fig. 2B), while showing significant down-regulation at 3-, 6-, 12- and 24-h post *V. alginolyticus* challenge (Fig. 2C). LPS challenge had no effect on the expression level of SpNPFII in hepatopancreas (Fig. 2E), while the expression level of SpNPFII in hepatopancreas was significantly up-regulated at the 3-, 6- and 12-h after *V. alginolyticus* challenge (Fig. 2F).

3.3. Sp-NPFin shows potent and broad-spectrum antimicrobial activity

Based on the bioinformatic analysis of the SpNPFII mature peptide, a truncated SpNPFII derived peptide was identified and named as Sp-NPFin. Sp-NPFin contained 45 amino acid residues (Fig. 1A), with a total hydrophobic ratio of 28%, a total net charge of +7, a calculated mass of 5.12 kDa and an estimated p*I* of 11.48. Sp-NPFin (purity >95%) was prepared using solid-phase chemical peptide synthesis and its antimicrobial activity was further examined using a panel of microorganisms. The MIC and MBC values measured are summarized in Table 2. Sp-NPFin displayed a broad antimicrobial spectrum, exerting potent activity against both Gram-negative (*E. coli*, *P. aeruginosa*, *P. stutzeri*, *P. fluorescens*, *S. flexneri*) and Gram-positive (*B. subtilis*, *C. glutamicum*, *S. aureus*) bacteria with MIC values ranging from 1.5–12 μM and MBC values lower than 24 μM. Sp-NPFin did not inhibit the growth of the fungi strains tested in the present study (*C. albicans*, *C. neoformans*, *P. pastoris* GS115), but showed profound inhibitory effect on the germination of mycotic spores (*Fusarium* spp., *Aspergillus* spp.) with MIC values of 3–48 μM. In addition, Sp-NPFin effectively inhibited the growth of several multi-drug resistant bacteria isolated from clinical samples (*e.g.*, *A. baumannii*, *K. pneumoniae*, *E. coli*, *P. aeruginosa*, *E. faecium* and *S. aureus*) with MIC values of 1.5–48 μM.

3.4. Killing kinetics of Sp-NPFin

Time-killing kinetic assays were applied to evaluate the bactericidal

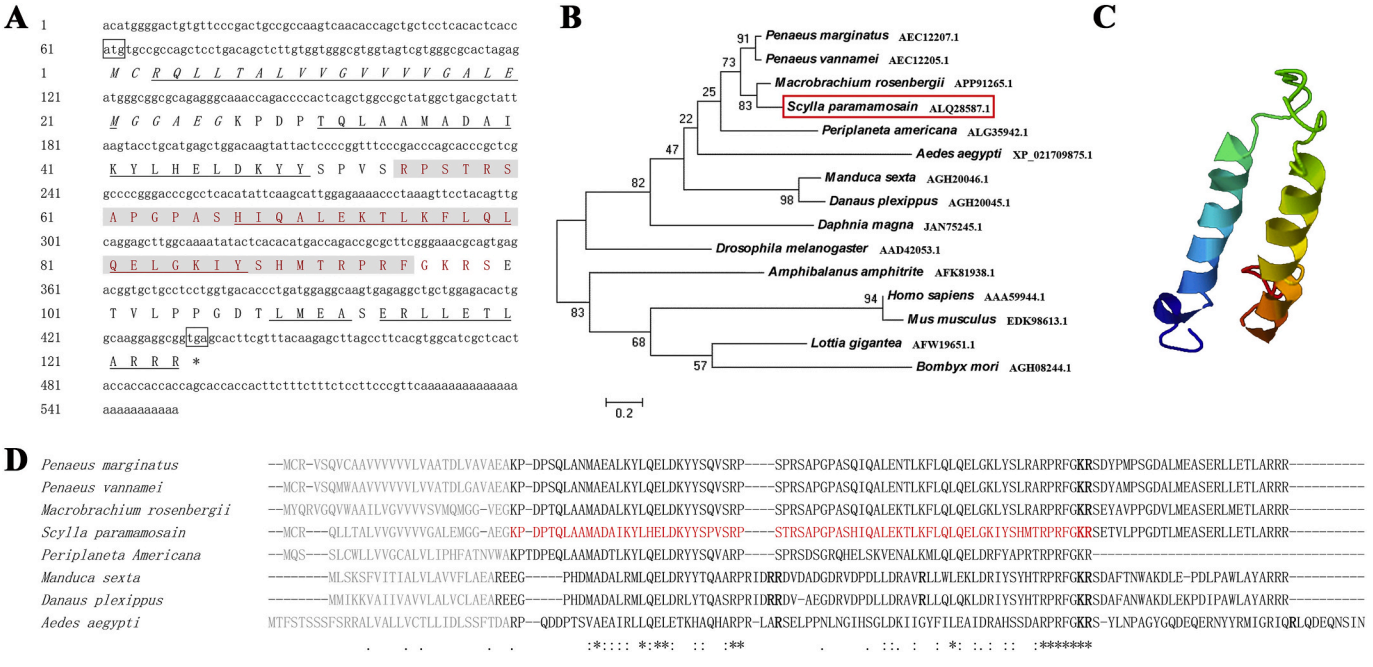

Fig. 1. Bioinformatics analysis and phylogenetic analysis of SpNPFII. The cDNA and deduced amino acid sequences of SpNPFII (A): the boxed sequence represents the initiation and stop codons; the predicted signal peptide is shown in Italics; underlined regions indicate the sequences that form α-helices; the predicted pancreatic hormone (PAH) domain is shown in red; the sequence of the synthetic Sp-NPFin is shaded. The phylogenetic tree based on the amino acid sequence of SpNPFII was generated using the neighbor-joining method (B). The protein structure of the SpNPFII mature peptide was predicted with the I-TASSER server (C). The alignment of the deduced amino acid sequences of invertebrate neuropeptide F-containing preprohormones was performed using Clustal X 2.1 software (D): dashes in the sequences indicate gaps, a star indicates amino acid residues that are identical in all sequences, a colon indicates amino acids that are highly conserved, and a single dot indicates amino acids that are conserved. The predicted signal peptide is shown in gray, the predicted mature peptide is shown in red, and the predicted prohormone convertase cleavage site is shown in bold. (For interpretation of the references to colour in this figure legend, the reader is referred to the web version of this article.)

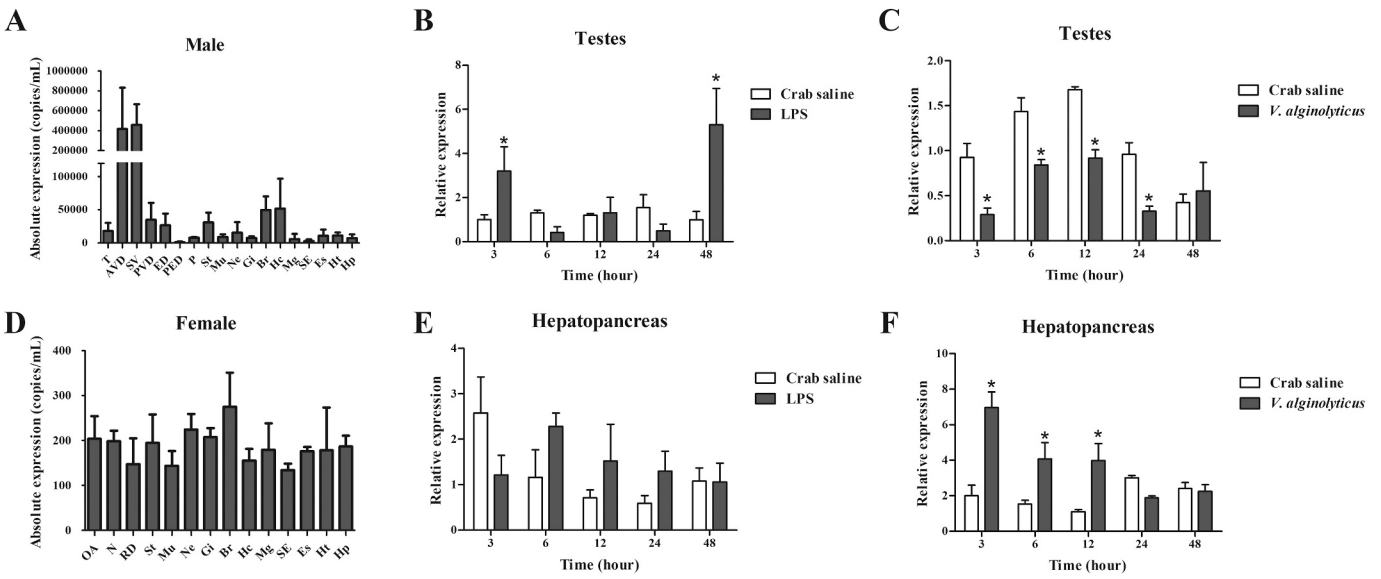

Fig. 2. Gene expression profiles of SpNPFII in *S. paramamosain*. The expression profile of SpNPFII in adult male (A) and female (D) crabs under natural status (n = 3) was determined by absolute qPCR. Data are presented as mean ± standard deviation (SD). *p < 0.05, one-way analysis of variance (ANOVA) and Tukey post-test. The relative expression of SpNPFII in male testes after LPS (B) and *V. alginolyticus* (C) challenges (n = 3), and in male hepatopancreas after LPS (E) and *V. alginolyticus* (F) challenges (n = 3) was examined. In panels B, C, E, and F, data are presented as mean ± SD. *p < 0.05, one-way analysis of variance (ANOVA) and Bonferroni post-test. Abbreviations: T, testis; AVD, anterior vas deferens; SV, seminal vesicle; PVD, posterior vas deferens; ED, ejaculatory duct; PED, posterior ejaculatory duct; P, penis; OA, ovary; S, spermathecae; RD, reproductive duct; Mu, muscle; Ne, thoracic ganglion; Gi, gills; Br, brain; Hc, hemocytes; Mg, midgut; SE, subcuticular epidermis; Es, eye stalk; Ht, heart; Hp, hepatopancreas; St, stomach.

efficiency of Sp-NPFin. When incubated with *S. aureus*, Sp-NPFin rapidly killed more than 90% of the bacteria in 6 min and eliminated all bacterial cells within around 30 min (Fig. 3A). Sp-NPFin showed no bactericidal effect against *P. aeruginosa* in the first 30 min of incubation, but it killed 99.99% of the *P. aeruginosa* cells after 2 h of incubation (Fig. 3B).

3.5. Binding properties of Sp-NPFin

To further investigate the antimicrobial mechanism of Sp-NPFin, we performed modified ELISA assays to assess its binding properties to different microbial surface molecules. As shown in Fig. 4A, Sp-NPFin could bind to LPS, LTA, PGN and glucan in a concentration-dependent manner. Scatchard plot analysis indicated that Sp-NPFin bound to LPS, LTA, PGN and glucan with calculated apparent dissociation constants (K_d) of 1.040, 0.583, 0.924 and 1.060 μM. These results suggested that Sp-NPFin had the strongest binding capacity with LTA, followed by LPS, PGN and glucan. In addition, immunofluorescent assays were carried out to determine the action site of Sp-NPFin on various microorganisms. The fluorescent signal of Sp-NPFin was detected on the cell membrane surface of *P. aeruginosa*, *S. aureus*, and spores of *A. niger* and *F. oxysporum*, but absent inside the cells (Fig. 4B).

3.6. Sp-NPFin induces morphological changes in microorganisms

In order to study the interaction between Sp-NPFin and the surface of microorganisms, SEM and TEM were used to observe morphological changes after Sp-NPFin treatment. After incubation with Sp-NPFin, the SEM images of *P. aeruginosa*, *S. aureus*, *A. niger* and *F. oxysporum* showed a significantly rougher surface, destruction of membrane integrity and even leakage of cellular contents (Fig. 5). TEM images further showed enlargement of intermembrane space (*P. aeruginosa*), destruction of both the inner and outer membrane (*S. aureus*) and leakage of cellular contents (Fig. 6). After SpNPFin treatment, the spore cell wall became

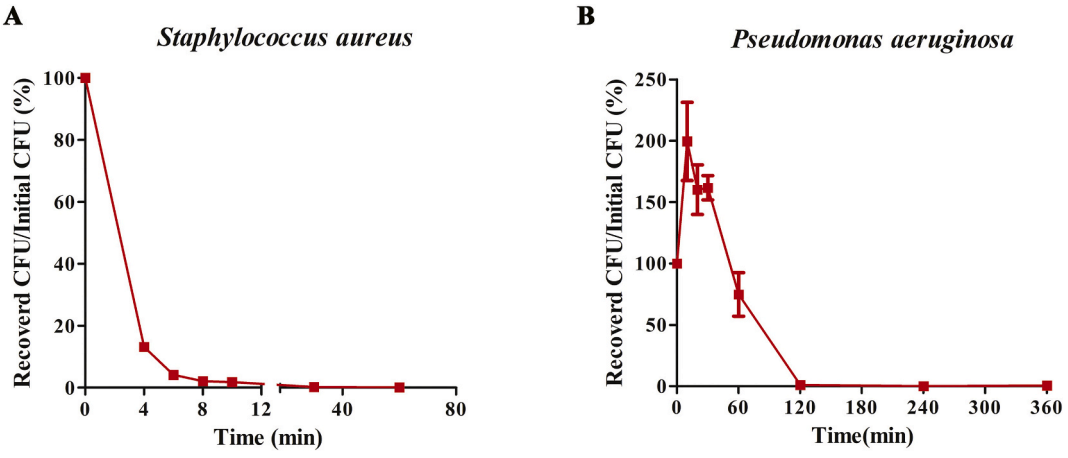

Fig. 3. Time-killing curves of *Staphylococcus aureus* and *Pseudomonas aeruginosa* treated with Sp-NPFin. The percentage of CFU is defined relative to the CFU obtained in the control (100% CFU at 0 min). Data are presented as mean ± standard deviation (SD) (n = 3).

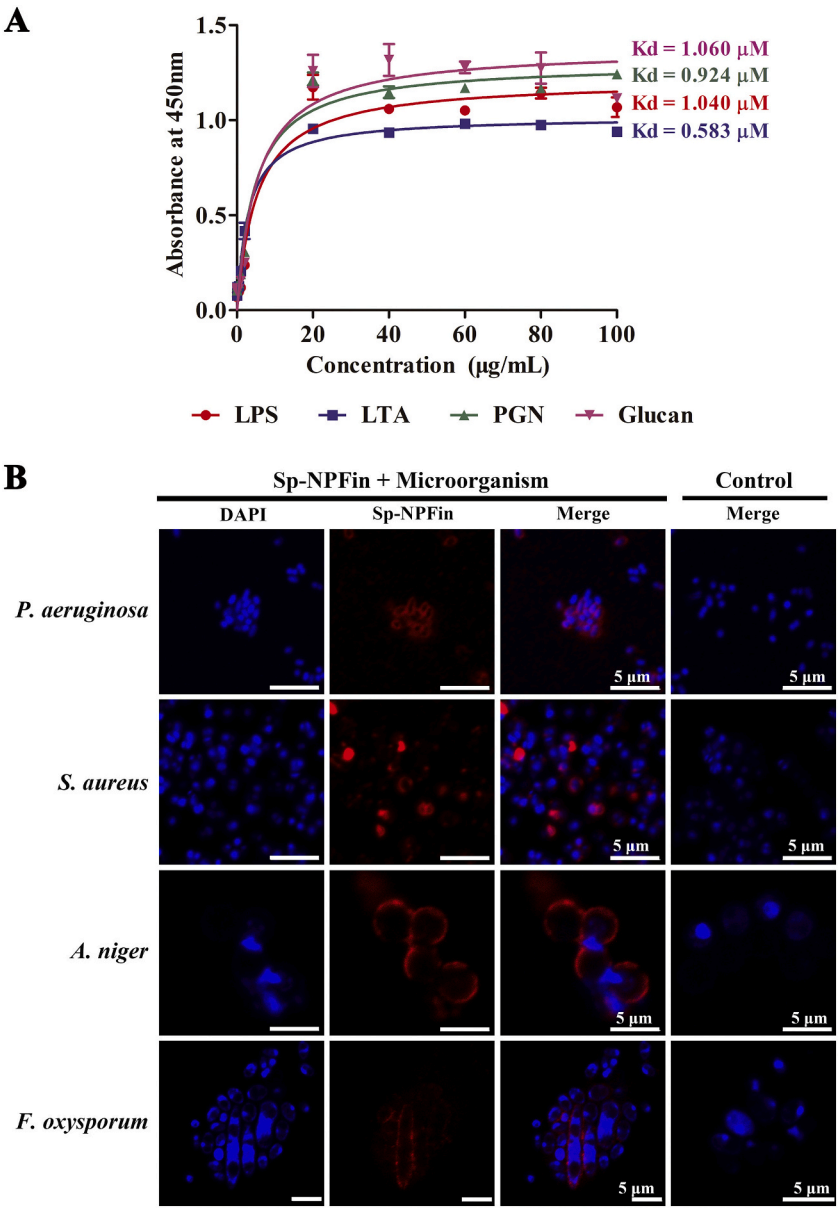

Fig. 4. Localization of Sp-NPFin in microorganisms. Binding properties of Sp-NPFin to LPS, LTA, PGN and glucan assessed by ELISA (A), data are presented as mean ± standard deviation (SD) (n = 3). Localization of Sp-NPFin in microorganisms was observed by confocal laser scanning microscopy (B). Only merged images are shown in the control groups.

thinner and disappeared, and the obvious destruction of organelles and leakage of spore contents were observed (Fig. 6).

3.7. *In vivo* protective effect of Sp-NPFin

To investigate the *in vivo* protective effect of Sp-NPFin, the *in vitro* cytotoxic effect of Sp-NPFin was first evaluated using crab hemocytes and mammalian cells (L02, HEK-293 T). As shown in Fig. 7A, Sp-NPFin showed no cytotoxic effect on primary cultured crab hemocytes in the concentration range of 0 to 24 μM, but inhibited cell growth at 48 μM. Additionally, Sp-NPFin had no cytotoxic effect on mammalian cells. To evaluate the *in vivo* activity of Sp-NPFin, mud crabs were challenged with *V. alginolyticus* at 2×10^5 CFU crab^{-1}, and Sp-NPFin injections (40 μg crab^{-1}) were given at 6 h post bacterial injection. As shown in Fig. 7, the survival rate of the crab saline injection group dropped to 40% at 36 h post bacterial challenge, while that of the Sp-NPFin injection group was around 60%. At 72 h post bacterial injection, Sp-NPFin significantly improved the survival rate of *V. alginolyticus*-challenged mud crabs (survival rate > 60%) compared to the control group (survival rate < 20%) ($p < 0.05$).

4. Discussion

Accumulating evidence suggests that the elimination of invading pathogens, termination of inflammation and restoration of host homeostasis depend on crosstalk between the neuroendocrine system and immune system (Souza-Moreira et al., 2011). The immune system protects organisms from infections; however, an imbalance of pro- and anti-inflammatory NPs would result in the loss of host homeostasis and can trigger inflammatory diseases. Therefore, NPs have attracted much attention in studies of the interaction between the immune system and the neuroendocrine system (Bedoui et al., 2007; Brogden et al., 2005). Mud crabs (*S. paramamosain*) rely on their innate immunity to defend against pathogenic infections, and their innate immune system has been extensively studied and reviewed (Chen and Wang, 2019). In recent years, many NPs (*e.g.* AST-A/B/C, NPF, sNPF, myosuppressin,

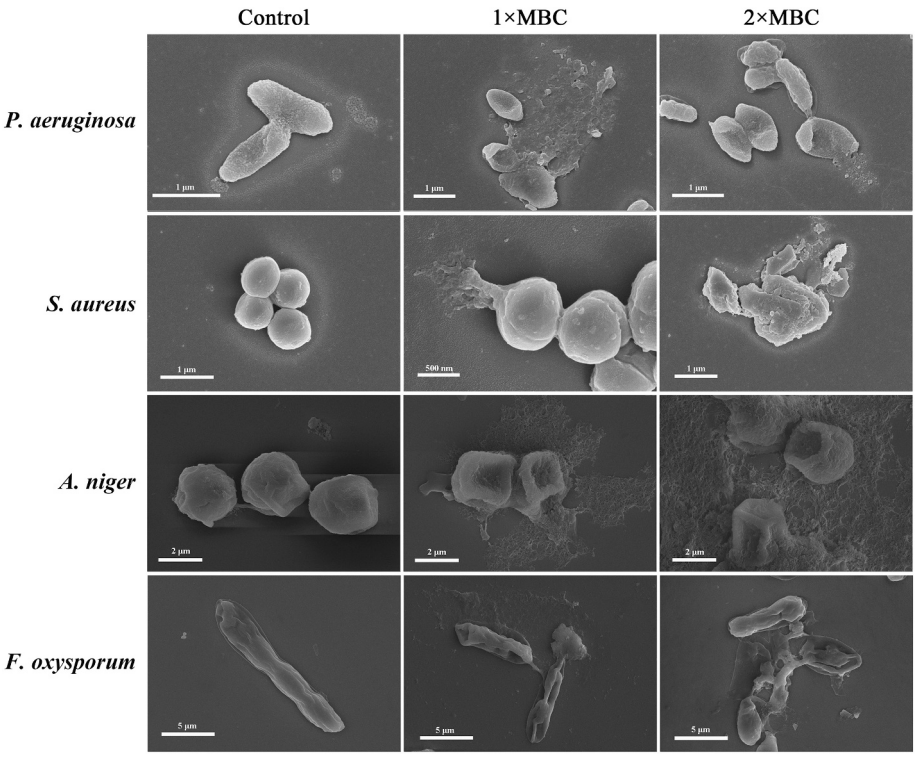

Fig. 5. Effect of Sp-NPFin on the membrane morphology of microorganisms. Exponential phase microbial cells (*P. aeruginosa* and *S. aureus*) and mycotic spores (*A. niger* and *F. oxysporum*) were suspended in culture media supplemented with PBS (control) or Sp-NPFin, and observed by a scanning electron microscopy (SEM).

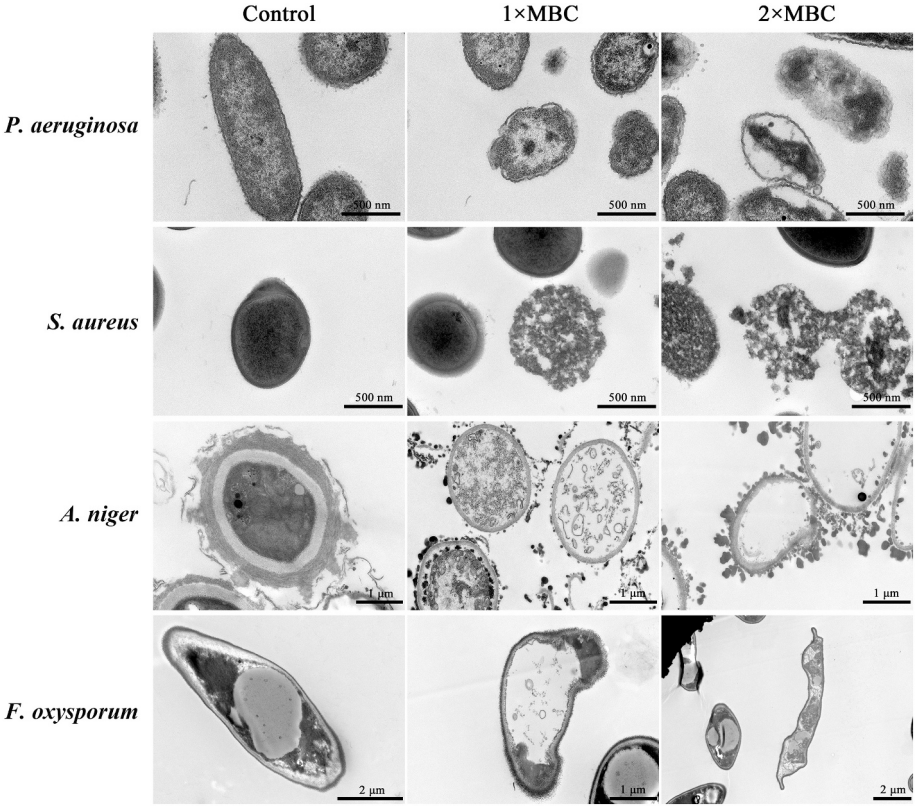

Fig. 6. Effect of Sp-NPFin on the morphology of microorganisms. Exponential phase microbial cells (*P. aeruginosa* and *S. aureus*) and mycotic spores (*A. niger* and *F. oxysporum*) were suspended in culture media supplemented with PBS (control) or Sp-NPFin, and observed by a transmission electron microscopy (TEM).

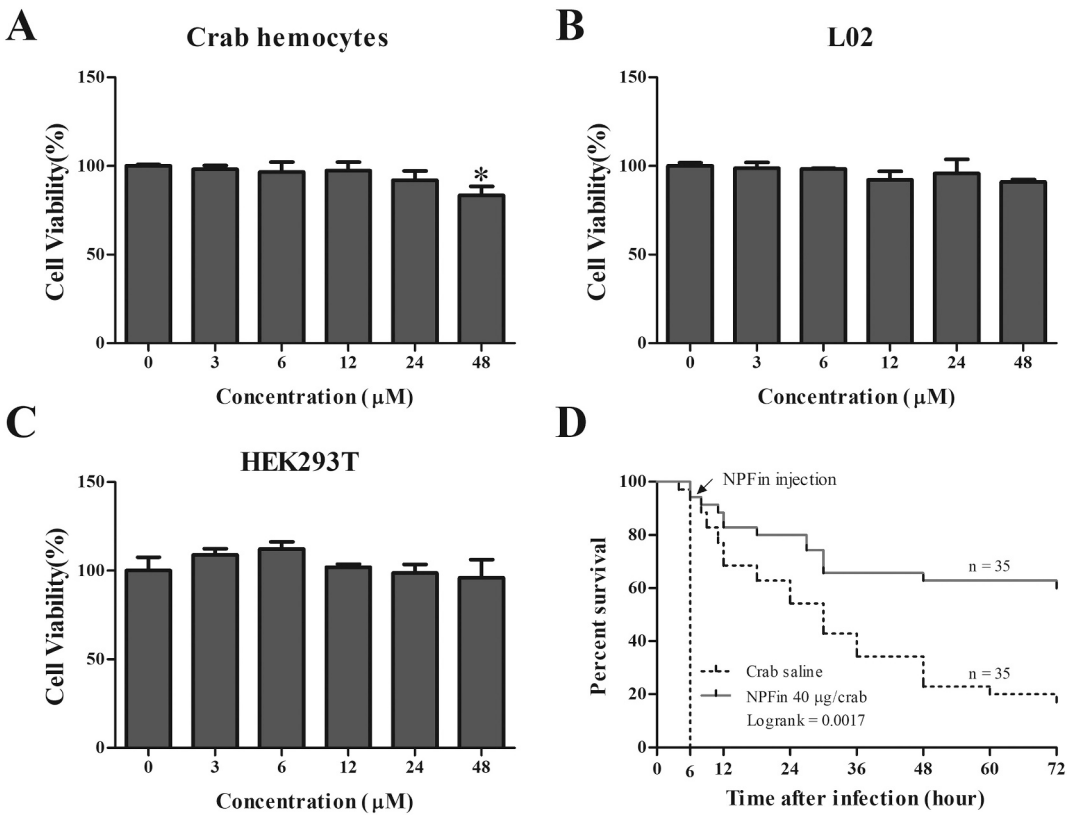

Fig. 7. *In vitro* cytotoxicity and the *in vivo* protective effect of Sp-NPFin. Cytotoxic effects of Sp-NPFin on crab hemocytes (A), L02 (B) and HEK-293 T (C) were determined by the MTS method. Data are presented as mean ± standard deviation (SD) (n = 3). *$p < 0.05$, one-way analysis of variance (ANOVA) and Dunnett post-test. The *in vivo* protective effect of Sp-NPFin was evaluated (D). Male crabs were challenged with *V. alginolyticus*, and Sp-NPFin was injected (40 μg crab^{-1}) at 6 h post bacterial challenge (n = 35 for each group). The survival curves were analyzed using the Kaplan-Meier Log rank test.

sulfakinin, neuroparsin, CHH) have been identified from transcriptome data and investigated for their roles in regulating female reproductive functions (Bao et al., 2015; Jiang et al., 2017; Liu et al., 2017; Ma et al., 2014). It is now clear that in *S. paramamosain*, NPF can repress vitellogenesis and oocyte maturation through the autocrine/paracrine pathway, while neuroparsin-1 may inhibit the production of vitellogenin (Liu et al., 2020; Lugo et al., 2013). However, little is known about the biological functions of NPs in the innate immunity of *S. paramamosain*. Herein, we identified an NPY family member, SpNPFII, in *S. paramamosain* and preliminarily explored its immune function. A truncated peptide of SpNPFII, Sp-NPFin, was identified and further proved to exert potent antimicrobial activity *in vitro* and *in vivo*, showing a protective effect against *V. alginolyticus* infection in mud crabs but a, low cytotoxic effects on crab hemocytes as well as mammalian cell lines.

Sexually different expressions of NPs have been observed in various animal species. In male rats and lizards (*Podaris hispanica*), NPY gene expression shows significant sexual dimorphism (Salom et al., 1994; Urban et al., 1993). In *Drosophila*, NPF expression is regulated in both a gender-nonspecific and a male-specific manner, which has a significant influence on the courtship activity of male *Drosophila* (Lee et al., 2006). In giant freshwater prawns (*Macrobrachium rosenbergii*), NPF is mainly expressed in females (Hadawale et al., 2019; Tinikul et al., 2017). It is interesting to note that there are also gender differences in SpNPFII gene expression (Fig. 1). Due to the complex relationship between gonads and hormones, gender differences of NPs may have important impacts on gender-specific behavioral processes or reproductive physiology. SpNPFII was highly expressed in two male gonadal tissues, the anterior vas deferens and seminal vesicle in *S. paramamosain*, while the overall expression level was lower in female crabs, suggesting that SpNPFII might play a role in activities related to male reproduction. However, the exact physiological function of SpNPFII requires further study.

Previous studies have shown that some NPs can respond to pathogenic and viral infections. For examples, expression levels of galanin and galanin type 1 receptors can be induced by *Salmonella typhimurium* infection (Lang and Kofler, 2011; Matkowskyj et al., 2009). The level of calcitonin gene-related peptide (CGRP) is significantly increased in the bronchoalveolar lavage fluid after MRSA strain USA300 infection (Baral et al., 2018). In the Hongkong oyster (*Crassostrea Hongkongensis*), expression of ChGnRH is significantly induced by *V. alginolyticus* and *V. parahaemolyticus* injection, and has been shown to participate in the immune system by promoting hemocytes phagocytosis and bacteria clearance through the cAMP-dependent PKA/PKC signaling pathway (Huang et al., 2019). Levels of kisspeptin, an NP encoded by Kiss1, were found to significantly increase during vesicular stomatitis virus (VSV) infection (Huang et al., 2018). In this study, the expression levels of SpNPFII showed significant changes under pathogen-related stimulations, indicating its involvement in the immune response of *S. paramamosain*. Mud crabs have an open vascular system and the hepatopancreas is immersed with the hemolymph; therefore, the hepatopancreas comes into direct contact with the *V. alginolyticus* injected into the crabs. The SpNPFII expression level in the hepatopancreas was significantly induced by *V. alginolyticus* challenge but not by LPS, suggesting that bacterial and LPS challenges have different ways of regulating the expression of SpNPFII. It was noted that SpNPFII expression in testes was suppressed after *V. alginolyticus* infection. In particular, testes are an immune-privileged organ; inflammation caused by bacterial or viral infections may perturb male fertility (Wang et al., 2019). Therefore, the down-regulation of SpNPFII expression after *V. alginolyticus*

challenge may be related to the negative regulatory system of immunity for maintaining immune homeostasis to ensure male fertility. Findings in this study revealed the complex *in vivo* regulatory pattern of SpNPFII under different statuses. Given the gender-specific differential expression pattern of SpNPFII in male mud crabs, future studies are required for comprehensive understanding of its roles in the male reproductive system and immune system.

Despite their traditional roles in signal transmission and modulation in the central and peripheral neural system, over the past decades some NPs have been thought to be related to AMPs and contribute to the formation of local barriers of defense against pathogens (Hancock and Sahl, 2006). Numerous studies have reported the direct *in vitro* antimicrobial activity of NPs (Augustyniak et al., 2012; Holub et al., 2011; Shimizu et al., 1998). It has been suggested that NPs could interfere with microbial pathogenesis by blocking microbial adhesion to host epithelial cells (Augustyniak et al., 2012), and some antimicrobial substances exert their protective effect by agglutination and entrapment of microbes (Crunkhorn, 2016).

Based on the bioinformatic analysis, we successfully identified a truncated peptide of SpNPFII, named as Sp-NPFin, with potent antimicrobial properties. Compared with the reviewed antimicrobial activity of NPs (Augustyniak et al., 2012), Sp-NPFin inhibited bacterial growth with relatively low MIC values (Table 2). For example, the MIC values of human NPY against *P. aeruginosa* and *S. aureus* are 11.7 μM to >370 μM and >117 μM respectively (Hansen et al., 2006), while that of Sp-NPFin were found to be 6–12 μM. Although Sp-NPFin did not affect the growth of yeasts, it effectively inhibited the germination of spores of *Fusarium* spp. and *Aspergillus* spp. *in vitro* (MIC values ranged from 1.5 to 48 μM) (Table 2). Most NPs share similar physiochemical features (*e.g.*, charge, hydropathicity, secondary structure) with AMPs. Like conventional AMPs, the majority of NPs utilize membrane-disruption as an important mode of action. For instance, loss of microbial membrane integrity has been observed after treatment with NPY, melanocyte-stimulating hormone (α-MSH) or adrenomedullin (Allaker et al., 2006; Madhuri et al., 2009; Shimizu et al., 1998). In our study, Sp-NPFin showed a strong binding affinity to microbial membrane related molecules (LPS, LTA, PGN, glucan). Immunofluorescence labeling analysis indicated that Sp-NPFin acted on microbial membranes, and electron microscopy further revealed the destruction of membrane integrity induced by Sp-NPFin in both bacteria and mycotic spores. It was thus deduced that the positively charged Sp-NPFin may exert its activity by electrostatic binding to the negatively charged microbial surface, destabilizing the phospholipid bilayer and further leading to disruption of the integrity of the microbial membrane. This direct membrane disruptive action in turn ensured the rapid killing kinetic of Sp-NPFin (Fig. 3). Interestingly, after Sp-NPFin treatment, the number of *P. aeruginosa* cells increased within the first 30 min. *P. aeruginosa* is a Gram-negative bacterium, and LPS is a key component of its asymmetric outer membrane. As shown in Fig. 4A, the binding affinity of Sp-NPFin to LPS is weaker than to LTA. Taken together, it was thus speculated that Sp-NPFin might need to interact with microbial membranes for a period of time and reach a certain threshold concentration on the membrane to acquire its bactericidal activity.

In order to obtain resistance against membrane-disrupting antimicrobial substances, microorganisms require extensive modification of anionic surface components in order to increase the number of positive charges. Redesigning membranes is unprofitable energetically for most of the pathogens; therefore, resistance to membranolytic peptides is very limited compared to that of the conventional antibiotics (Peschel and Sahl, 2006). In addition to membrane disruptive action mode, some NPs exert their antimicrobial activity by interfering with intracellular metabolic functions. For example, α-MSH binds to a membrane receptor and mediates the induction of cyclic adenosine monophosphate (cAMP). The rise in cAMP in turn affects the regulatory mechanisms of yeast, leading to cell death (Catania et al., 2006; Cutuli et al., 2000). Adrenomedullin induces cell wall disruption in *E. coli* and interferes in cell wall division in *S. aureus* (Allaker et al., 2006). Findings in the work here demonstrated that Sp-NPFin can rapidly kill bacteria and inhibit spore germination by membrane destruction, which makes it a promising antibiotic substitute. Despite all the advantages of Sp-NPFin, it remains to be further evaluated whether it has other action modes and whether microorganisms would develop resistance to Sp-NPFin treatment.

In the present study, the *in vivo* activity of Sp-NPFin was characterized through bacterial challenge experiments. Although Sp-NPFin had no inhibitory effect on *V. alginolyticus*, injection of Sp-NPFin post *V. alginolyticus* challenge significantly improved the survival rate of crabs, suggesting that Sp-NPFin had a favorable *in vivo* protective effect against bacterial infection. Moreover, Sp-NPFin showed no cytotoxic effect on crab hemocytes and mammalian cells. In recent years, application of marine-derived bioactive substances in medication and animal welfare has attracted much attention. Promising candidates identified from mud crabs (*e.g.* Sphistin, SpHyastatin, scyreprocin) have been proven to have strong antimicrobial activity against pathogenic microorganisms *in vitro*, improving the survival rate of the animals under infection through *in vivo* treatment (Ma et al., 2017; Shan et al., 2016; Yang et al., 2020). Our present work provided fundamental data showing that Sp-NPFin is a bio-friendly and effective antimicrobial agent, which could have applications in aquaculture, veterinary practices and medication. In the view of the fact that Sp-NPFin did not inhibit the growth of *V. alginolyticus in vitro*, whether Sp-NPFin injected into the mud crabs can resist the challenge of *V. alginolyticus* by regulating the neuroendocrine system or immune system remains to be further studied.

5. Conclusion

In conclusion, the newly characterized neuropeptide SpNPFII showed a gender-specific differential expression pattern and significantly responded to bacterial challenge in *S. paramamosain*. Sp-NPFin, a truncated 45-amino acid peptidewas identified and shown to exert potent antimicrobial activity as well as the effective inhibition of spore germination. The synthetic Sp-NPFin effectively killed microbes by directly interacting with their membranes and conducting a membrane disruptive action mode against bacteria and mycotic spores. Moreover, Sp-NPFin improved the survival rate of mud crabs under *V. alginolyticus* challenge, and showed no cytotoxic effect on crab hemocytes and mammalian cells. The findings in the present study revealed the expression profile and immune response of SpNPFII under bacterial infection, which for the first time depicted the possible roles of NPs in the immune system of *S. paramamosain*. In addition, the identification and demonstration of the *in vitro* and *in vivo* antimicrobial activity of Sp-NPFin further provided an important reference for the development and application of NPs in antimicrobial agents.

Author contributions

F. C. and K. J. W: Conceptualization; Funding acquisition; Project administration; Supervision; Writing - review & editing. H. Z and Y. Y: Data curation; Formal analysis; Investigation; Methodology; Writing - original draft. X. Z and Y. L: Investigation; Methodology.

Declaration of Competing Interest

The authors declare that the research was conducted in the absence of any commercial or financial relationships that could be construed as a potential conflict of interest.

Acknowledgments

This study was supported by grants (grant # 41806162 and grant # U1805233) from the National Natural Science Foundation of China (NSFC), the Fundamental Research Funds from Central Universities (grant # 20720180100 and grant # 20720190109), the Fujian Marine

Economic Development 395 Subsidy Fund Project (Grant # FJHJF-L-2019-1) from the Fujian Ocean and Fisheries Department and a grant (# 3502Z20203012) from the Xiamen Science and Technology Planning Project.

References

Allaker, R.P., Grosvenor, P.W., Mcanerney, D.C., Sheehan, B.E., Srikanta, B.H., Pell, K., Kapas, S., 2006. Mechanisms of adrenomedullin antimicrobial action. Peptides 27, 661–666.

Augustyniak, D., Nowak, J., Lundy, T.F., 2012. Direct and indirect antimicrobial activities of neuropeptides and their therapeutic potential. Curr. Protein Pept. Sci. 13, 723–738.

Bao, C., Yang, Y., Huang, H., Ye, H., 2015. Neuropeptides in the cerebral ganglia of the mud crab, Scylla paramamosain: transcriptomic analysis and expression profiles during vitellogenesis. Sci. Rep. 5, 17055.

Baral, P., Umans, B.D., Li, L., Wallrapp, A., Bist, M., Kirschbaum, T., Yibing, W., Zhou, Y., Kuchroo, V.K., Burkett, P.R., Yipp, B.G., Liberles, S.D., Chiu, I.M., 2018. Nociceptor sensory neurons suppress neutrophil and γδ Tcell responses in bacterial lung infections and lethal pneumonia. Nat. Med. 24, 417–426.

Bedoui, S., Hörsten, S.v., Gebhardt, T., 2007. A role for neuropeptide Y (NPY) in phagocytosis: implications for innate and adaptive immunity. Peptides 28, 373–376.

Botelho, M., Cavadas, C., 2015. Neuropeptide Y: an anti-aging player? Trends Neurosci. 38, 701–711.

Brogden, K.A., Guthmiller, J.M., Salzet, M., Zasloff, M., 2005. The nervous system and innate immunity: the neuropeptide connection. Nat. Immunol. 6, 558–564.

Catania, A., Colombo, G., Rossi, C., Carlin, A., Sordi, A., Lonati, C., Turcatti, F., Leonardi, P., Grieco, P., Gatti, S., 2006. Antimicrobial properties of α-MSH and related synthetic melanocortins. Sci. World J. 6, 1241–1246.

Chang, M.M., Leeman, S.E., Niall, H.D., 1971. Amino-acid sequence of substance P. Nat. New Biol. 232, 86–87.

Chen, F., Wang, K., 2019. Characterization of the innate immunity in the mud crab *Scylla paramamosain*. Fish Shellfish Immunol. 93, 436–448.

Chen, F.Y., Lui, H.P., Bo, J., Ren, H.L., Wang, K.J., 2010. Identification of genes differentially expressed in hemocytes of *Scylla paramamosain* in response to lipopolysaccharide. Fish Shellfish Immunol. 28, 167–177.

Chen, H.M., Chan, S.C., Lee, J.C., Chang, C.C., Jack, R.W., 2003. Transmission electron microscopic observations of membrane effects of antibiotic Cecropin B on *Escherichia coli*. Microsc. Res. Tech. 62, 423–430.

Christie, A.E., Chapline, M.C., Jackson, J.M., Dowda, J.K., Hartline, N., Malecha, S., Lenz, R.P.H., 2011. Identification, tissue distribution and orexigenic activity of neuropeptide F (NPF) in penaeid shrimp. J. Exp. Biol. 214, 1386–1396.

Crunkhorn, S., 2016. Alzheimer disease: antimicrobial role of amyloid-β. Nat. Rev. Drug Discov. 15, 456.

Cutuli, M., Cristiani, S., Lipton, J.M., Catania, A., 2000. Antimicrobial effects of α-MSH peptides. J. Leukoc. Biol. 67, 233–239.

Deepika, A., Makesh, M., Rajendran, K.V., 2014. Development of primary cell cultures from mud crab, *Scylla serrata*, and their potential as an in vitro model for the replication of white spot syndrome virus. In Vitro Cell Dev. Biol. Anim. 50, 406–416.

Delgado, M., Ganea, D., 2008. Anti-inflammatory neuropeptides: a new class of endogenous immunoregulatory agents. Brain Behav. Immun. 22, 1146–1151.

Duarte-Neves, J., De Almeida, L.P., Cavadas, C., 2016. Neuropeptide Y (NPY) as a therapeutic target for neurodegenerative diseases. Neurobiol. Dis. 95, 210–224.

Hadawale, K.N., Sawant, N.S., Sagarkar, S., Sakharkar, A.J., Bhargava, S.Y., 2019. Sex-specific distribution of neuropeptide Y (NPY) in the brain of the frog, *Microhyla ornata*. Neuropeptides 74, 1–10.

Hancock, R.E.W., Sahl, H.G., 2006. Antimicrobial and host-defense peptides as new anti-infective therapeutic strategies. Nat. Biotechnol. 24, 1551–1557.

Hansen, C.J., Burnell, K.K., Brogden, K.A., 2006. Antimicrobial activity of substance P and neuropeptide Y against laboratory strains of bacteria and oral microorganisms. J. Neuroimmunol. 177, 215–218.

Holub, B.S., Rauch, I., Radner, S., Sperl, W., Hell, M., Kofler, B., 2011. Effects of galanin message-associated peptide and neuropeptide Y against various non-albicans *Candida* strains. Int. J. Antimicrob. Agents 38, 76–80.

Huang, H., Xiong, Q., Wang, N., Chen, R., Ren, H., Stefan, S., Han, H., Liu, M., Qian, M., Du, B., 2018. Kisspeptin/GPR54 signaling restricts antiviral innate immune response through regulating calcineurin phosphatase activity. Sci. Adv. 4 (eaas9784).

Huang, Q., Li, Q., Chen, H., Lin, B., Chen, D., 2019. Neuroendocrine immune-regulatory of a neuropeptide ChGnRH from the Hongkong oyster, *Crassostrea Hongkongensis*. Fish Shellfish Immunol. 93, 911–916.

Jenwitheesuk, A., Park, S., Wongchitrat, P., Tocharus, J., Mukda, S., Shimokawa, I., Govitrapong, P., 2017. Comparing the effects of melatonin with caloric restriction in the hippocampus of aging mice: involvement of Sirtuin1 and the FOXOs pathway. Neurochem. Res. 43, 153–161.

Jiang, Q., Bao, C., Yang, Y.N., Liu, A., Ye, H., 2017. Transcriptome profiling of claw muscle of the mud crab (*Scylla paramamosain*) at different fattening stages. PLoS One 12, e0188067.

Lang, R., Kofler, B., 2011. The galanin peptide family in inflammation. Neuropeptides 45, 1–8.

Lee, G., Bahn, J.H., Park, J.H., 2006. Sex- and clock-controlled expression of the neuropeptide F gene in *Drosophila*. Proc. Natl. Acad. Sci. U. S. A. 103, 12580–12585.

Lin, W., Yang, J., He, X., Mo, G., Jing, H., Yan, X., Lin, D., Ren, L., 2013. Structure and function of a potent lipopolysaccharide-binding antimicrobial and anti-inflammatory peptide. J. Med. Chem. 9, 3546–3556.

Liu, J., Liu, A., Liu, F., Huang, H., Ye, H., 2020. Role of neuroparsin 1 in vitellogenesis in the mud crab, *Scylla paramamosain*. Gen. Comp. Endocrinol. 285, 113248.

Liu, S., Chen, G., Xu, H., Zou, W., Yan, W., Wang, Q., Deng, H., Zhang, H., Yu, G., He, J., 2017. Transcriptome analysis of mud crab (*Scylla paramamosain*) gills in response to mud crab reovirus (MCRV). Fish Shellfish Immunol. 60, 545–553.

Livak, K.J., Schmittgen, T.D., 2001. Analysis of relative gene expression data using real-time quantitative PCR and the $2^{-\Delta\Delta CT}$ method. Methods 25, 402.

Lu, Y., Ho, R., Lim, T.K., Kuan, W.S., Goh, D.Y.T., Mahadevan, M., Sim, T.B., Van Bever, H.P.S., Larbi, A., Ng, T.P., 2015. Neuropeptide Y may mediate psychological stress and enhance TH2 inflammatory response in asthma. J. Allergy Clin. Immunol. 135, 1061–1063 (e1064).

Lugo, J.M., Carpio, Y., Morales, R., Rodríguez-Ramos, T., Ramos, L., Estrada, M.P., 2013. First report of the pituitary adenylate cyclase activating polypeptide (PACAP) in crustaceans: conservation of its functions as growth promoting factor and immunomodulator in the white shrimp *Litopenaeus vannamei*. Fish Shellfish Immunol. 35, 1788–1796.

Ma, H., Ma, C., Li, S., Wei, J., Li, X., Liu, Y., Ma, L., Cynthia, G., 2014. Transcriptome analysis of the mud crab (*Scylla paramamosain*) by 454 deep sequencing: assembly, annotation, and marker discovery. PLoS One 9, e102668.

Ma, X.W., Hou, L., Chen, B., Fan, D.Q., Chen, Y.C., Yang, Y., Wang, K.J., 2017. A truncated Sph12-38 with potent antimicrobial activity showing resistance against bacterial challenge in *Oryzias melastigma*. Fish Shellfish Immunol. 67, 561–570.

Madhuri T., Shireen, Venugopal, S.K., Ghosh, D., Gadepalli, R., Dhawan, B., Mukhopadhyay, K., 2009. *In vitro* antimicrobial activity of alpha-melanocyte stimulating hormone against major human pathogen *Staphylococcus aureus*. Peptides 30, 1627–1635.

Matkowskyj, K., Royan, S.V., Blunier, A., Hecht, G., Rao, M., Benya, R.V., 2009. Age-dependent differences in galanin-dependent colonic fluid secretion after infection with *Salmonella typhimurium*. Gut. 58, 1201–1206.

Matsuda, K., Kang, K.S., Sakashita, A., Yahashi, S., Vaudry, H., 2015. Behavioral effect of neuropeptides related to feeding regulation in fish. Ann. N. Y. Acad. Sci. 1220, 117–125.

Maule, A.G., Shaw, C., Halton, D.W., Thim, L., Johnston, C.F., Fairweather, I., Buchanan, K.D., 1991. Neuropeptide F: a novel parasitic flatworm regulatory peptide from *Moniezia expansa* (Cestoda: Cyclophyllidea). Parasitology 102, 309–316.

Merighi, A., 2011. Neuropeptides: methods and protocols. Methods Mol. Biol. 843–849.

Metz-Boutigue, M.H., Kieffer, A.E., Goumon, Y., Aunis, D., 2003. Innate immunity: involvement of new neuropeptides. Trends Microbiol. 11, 585–592.

Nässel, D.R., Wegener, C., 2011. A comparative review of short and long neuropeptide F signaling in invertebrates: any similarities to vertebrate neuropeptide Y signaling? Peptides 32, 1335–1355.

Nässel, D.R., Zandawala, M., 2019. Recent advances in neuropeptide signaling in Drosophila, from genes to physiology and behavior. Prog. Neurobiol. 179, 101607.

Nguyen, M.D., Julien, J.P., Rivest, S., 2002. Innate immunity: the mssing link in neuroprotection and neurodegeneration? Nat. Rev. Neurosci. 3, 216–227.

Pain, S., Bodard, S., Gulhan, Z., Vergote, J., Chalon, S., Gaillard, A., 2019. Inflammatory process in Parkinson disease: neuroprotection by neuropeptide Y. Fundam. Clin. Pharmacol. 33, 544–548.

Peschel, A., Sahl, H., 2006. The co-evolution of host cationic antimicrobial peptides and microbial resistance. Nat. Rev. Microbiol. 4, 529–536.

Qiao, K., Zhang, Y.Q., Wang, S.P., Zhe, A.N., Hao, H., Chen, F.Y., Peng, H., 2014. The optimization of primary hemocyte culture of *Scylla paramamosain*. China Anim. Husbandry Vet. Med. 41, 145–149.

Ramos, E.J., Meguid, M.M., Campos, A.C., Coelho, J.C., 2005. Neuropeptide Y, alpha-melanocyte-stimulating hormone, and monoamines in food intake regulation. Nutrition 21, 269–279.

Reichmann, F., Holzer, P., 2015. Neuropeptide Y: a stressful review. Neuropeptides 55, 99–109.

Salom, S., Font, C., Martínez-García, F., 1994. Seasonal sexually dimorphic distribution of neuropeptide Y-like immunoreactive neurons in the forebrain of the lizard *Podarcis hispanica*. J. Chem. Neuroanat. 7, 217–225.

Sanz, J.A., Aidy, S.E., 2019. Microbiota and gut neuropeptides: a dual action of antimicrobial activity and neuroimmune response. Psychopharmacology 236, 1597–1609.

Shan, Z., Zhu, K., Peng, H., Chen, B., Liu, J., Chen, F., Ma, X., Wang, S., Qiao, K., Wang, K., 2016. The new antimicrobial peptide SpHyastatin from the mud crab *Scylla paramamosain* with multiple antimicrobial mechanisms and high effect on bacterial infection. Front. Microbiol. 7, 1140.

Shao, L.W., Niu, R., Liu, Y., 2016. Neuropeptide signals cell non-autonomous mitochondrial unfolded protein response. Cell Res. 026, 1182–1196.

Sharma, R., Sahota, P., Thakkar, M.M., 2018. Melatonin promotes sleep in mice by inhibiting orexin neurons in the perifornical lateral hypothalamus. J. Pineal Res. 65, e12498.

Shimizu, M., Shigeri, Y., Yoshikawa, S., Yumoto, N., 1998. Enhancement of antimicrobial activity of neuropeptide Y by N-terminal truncation. Antimicrob. Agents Chemother. 42, 2745–2746.

Souza-Moreira, L., Campos-Salinas, J., Caro, M., Gonzalez-Rey, E., 2011. Neuropeptides as pleiotropic modulators of the immune response. Neuroendocrinology 94, 89–100.

Takei, Y., 2016. Handbook of Hormones. Science, Elsevier, San Diego.

Tinikul, Y., Engsusophon, A., Kruangkum, T., Thongrod, S., Ruchanok, S., 2017. Neuropeptide F stimulates ovarian development and spawning in the female giant freshwater prawn, *Macrobrachium rosenbergii*, and its expression in the ovary during ovarian maturation cycle. Aquaculture 496, 128–136(129).

Urban, J.H., Bauer-Dantoin, A.C., Levine, J.E., 1993. Neuropeptide Y gene expression in the arcuate nucleus: sexual dimorphism and modulation by testosterone. Endocrinology 132, 139–145.

Wang, F., Chen, R., Han, D., 2019. Innate immunity defense in the male reproductive system and male fertility. In: Saxena, S.K., Prakash, H. (Eds.), Innate Immunity in Health and Disease. IntechOpen Limited, London, UK.

Woods, T.A., Min, D., Carmody, A., Peterson, K.E., 2016. Neuropeptide Y negatively influences monocyte recruitment to the central nervous system during retrovirus infection. J. Virol. 90, 2783–2793.

Yang, Y., Chen, F., Chen, H.-Y., Peng, H., Hao, H., Wang, K.-J., 2020. A novel antimicrobial peptide scyreprocin from mud crab *Scylla paramamosain* showing potent antifungal and anti-biofilm activity. Front. Microbiol. 11, 1589.